An investigation into the effect of burial depth ratio, pipe size, and soil type, in soil-pipeline interaction in sand

K. Badv[1] & K. E. Daryani[2]
Department of Civil Engineering, Urmia University, Urmia, Iran

ABSTRACT
The effect of burial depth ratio, pipe size, and soil properties were investigated in upward and lateral soil-pipeline interaction in sand. This paper investigates the response of buried pipelines in sand to transverse PGD. Available analytical solutions provide a wide range of predicted peak dimensionless forces but there is limited information regarding the transition of the peak dimensionless force from shallow to deep embedment conditions. There are large uncertainly in the true values since the bounds established by the analytical solutions are large. In order to find the solution and to investigate its failure envelope in oblique direction, the numerical modeling of soil-pipe interaction is performed for different conditions. The study concludes that the effects of burial depth, pipe size, and soil type, must be taken into account to properly estimate the bearing capacity factors for sand in horizontal and vertical (upward) directions.

RÉSUMÉ
L'effet du taux d'enfouissement en profondeur, la taille du tube, et les propriétés du sol ont été étudiés dans le sol vers le haut et latéral interaction oléoduc dans le sable. Ce document examine la réponse des canalisations enfouies dans le sable transversal à un PDS. Les solutions analytiques disponibles fournissent une large gamme de prédire forces maximales sans dimension, mais il ya des informations limitées concernant le passage du pic de force sans dimension de peu profondes à des conditions d'encastrement de profondeur. Il existe de grandes incertitudes dans l'vraies valeurs depuis les limites établies par les solutions d'analyse sont importants. Afin de trouver la solution et d'enquêter sur l'échec de son enveloppe en direction oblique, la modélisation numérique de l'interaction sol-tuyau est effectuée pour différentes conditions. L'étude conclut que les effets de profondeur d'enfouissement, la taille du tube, et le type de sol, doit être pris en compte pour estimer correctement les facteurs de capacité portante pour le sable dans les directions horizontale et verticale (vers le haut).

1 INTRODUCTION

There are several publications and reports from all over the world that discuss the severe damages caused by the failure of water and gas pipelines during or after the occurrence of high-intensity earthquakes. Seismic hazards have been classified as being either permanent ground deformation hazards or wave propagation hazards (O'Rourke & Liu, 1999). In particular, pipe damage concentrated in the areas of permanent ground deformation resulting from slope failures, earthquake-induced faulting, landslide and liquefaction, urban excavation and tunnelling, and excessive ground settlement. Under such events, loads are induced in a pipeline by relative motion between the pipeline and surrounding soil. The soil movement can be in transverse (perpendicular to the pipeline axis) or longitudinal (parallel to the pipeline axis) direction or complex of them relative pipe installation.

In the current state-of-practice (e.g., Committee on Gas and Liquid Fuel Lifelines of ASCE 1984; ALA 2005), the pipeline is generally simplified as a beam, while pipe-soil interaction is represented by soil springs in the axial (or longitudinal), transverse horizontal and vertical directions, as shown in Figure 1. This simplification is derived from the concept of sub-grade reaction originally proposed by Winkler (1867). Winkler-type soil models are unable to describe complicated soil behaviour, such as dilatancy, stress path dependency and, to some extent, strain hardening or softening and failure mechanism of surrounding soil. The springs describing the soil resistance to deformation are usually assumed independent of one another. Therefore, no connection between adjacent soil zones is considered.

ALA defined the peak transverse yield load per unit length of pipe in sand as follows:

$$F_{peak} = \bar{\gamma} H N_q D \qquad [1]$$

Where $\bar{\gamma}$ is the soil effective unit weight; H is the soil depth to the centerline of pipe; D is the pipe outer diameter and Nq is the transverse horizontal or vertical bearing capacity factor adopted from Hansen (1961) or Rowe and Davis (1982).

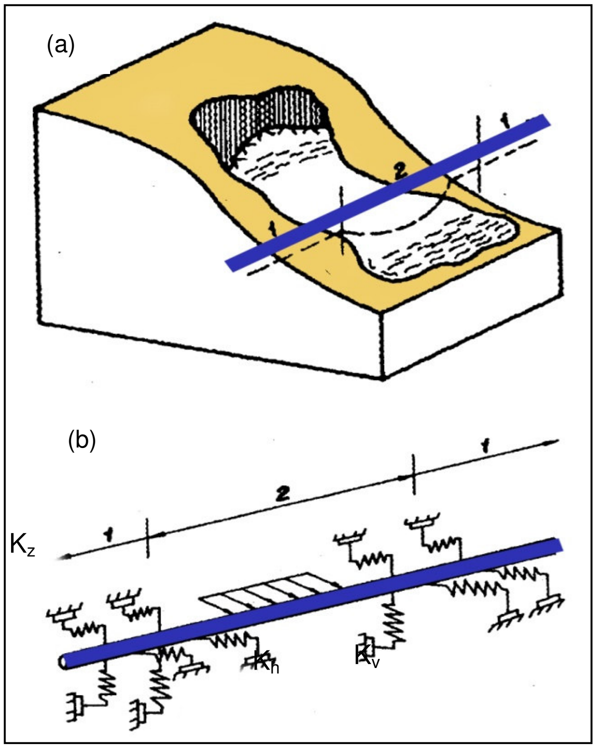

Figure 1. (a) Pipeline displacement due to PGD, (b) Winkler type spring soil-pipe model (Winkler, 1867)

2 SOIL-PIPELINE INTERACTION

The soil around a pipeline plays a very important role in relation to its seismic behavior; if it is cohesive soil, the softer it is, the greater differential settlements there will be due to consolidation or higher amplification effects; if it is granular material, the probability of liquefaction becomes higher the looser it is. Nevertheless, when we talk about soil-pipe interaction, it is supposed that the soil will not fail, but the soil displacements will produce friction-like forces at the soil-pipe interface. An elasto-plastic model is often adopted for the force-deformation behavior at soil-pipeline interface (O'Rourke et al, 1995). This model is fully defined by two parameters: the maximum axial force per unit length at the soil pipe interface F_m and the relative displacement at which slippage between pipe and soil occurs.

Practical engineering solutions, which often use structural numerical analysis, are advantageous in terms of the simplicity, functionality and utility for conducting preliminary assessment of pipeline integrity and parametric analysis. The procedures, however, are limited by the assumptions and idealizations considered. Furthermore, analytical difficulties are encountered for pipe-soil interaction considering non-uniform boundary conditions, spatial variation in characteristics of the pipeline and soil media, large amplitude, accumulated or cyclic deformational loading mechanisms and nonlinear material behaviour. For these issues, continuum models using finite element or finite difference methods are robust and comprehensive numerical tools and can address a number of limitations in reproducing soil constitutive behavior, soil deformation mechanisms (e.g. shear load transfer) and soil-pipe interaction (e.g. variable circumferential or longitudinal pressure distribution).

This work presents a continuum model of pipe buried in soil. We used the finite difference method to analyze lateral and upward soil-pipe interaction for large diameter pipes. Several aspects related to pipe-soil interaction involving large relative displacements that cannot be captured by the current state-of-practice structural models, are presented and analyzed based on results of numerical modeling. These include: (1) effects of the soil failure mechanism on interaction forces, (2) effects of pipe diameter, (3) effects of burial depth ratio, and (4) effects of soil properties on interaction forces and pipe loading capacity.

3 PREVIOUS STUDIES

Previous works on soil-pipeline interaction induced by lateral and upward movements mainly focus on the prediction of the maximum horizontal and vertical soil forces and the force-displacement relations. There are a few publications to describe the effect of some parameters to the loading.

The following are examples of such analyses: Popescu et al. (1997) developed a 2D finite element model in ABAQUS and simulated the full-scale performed at C-CORE. With the use of Mohr-Coulomb model as soil constitutive model, the numerical model showed a good agreement with test results in term of peak load and mobilization of load on the pipe. Popescu and Nobahar (2003) studied the effect of groundwater in soil-pipe interaction using ABAQUS/Std. Using the experimental results of Trautmann and O'Rourke (1983) for tests in sand with overburden of 2 to 11, Yimsiri et al. (2004) calibrated a finite element model to investigate soil behavior in deep embedment. They used two different constitutive models: Mohr-Coulomb model and Nor-Sand model. They extended the result of numerical model to overburden ratios of 100 and suggested limitation values for dimensionless load for different friction angles. Guo and Stolle (2005) collected the result of previous experiments to investigate the effect of different parameters on lateral soil loads on the pipe using ABAQUS software and Mohr-Coulomb soil model with constant dilation angle and constant friction angle as initial constitutive model. They studied the effect of geometrical factors and performed sensitivity analysis of soil parameters for pipes buried in shallow conditions. They suggested a series of relations to account for the effect of pipe diameter, soil dilatancy, and burial depth. Applications of suggested relations indicates that the dimensionless soil loads on a pipe with outside diameter of 30 mm are about 80% more than that of a pipe with outside diameter of 300 mm, buried in the same material and with the same overburden ratio.

In the above review, all of the numerical models conducted by ABAQUS software pancakes with some limitations. There are a few investigations of soil-pipe interaction using other numerical methods.

4 NUMERICAL MODEL

The finite difference analysis package, FLAC 2D V4.0 (Fast Lagrangian Analysis of Continua), was chosen for the numerical analysis. Since in FLAC there is no need to form a stiffness matrix, it is a trivial matter to update coordinates at each time step in large-strain mode. The incremental displacements are added to the coordinates so that the, grid moves and deforms with the material it represents. In this 2-D approach, beam elements are used to represent a rigid pipe section and the nodes of pipe interface elements are attached to the beam nodes to represent the possibility of slippage between the pipe and the soil. The model used in this study, was calibrated and validated based on both experimental data and finite element model. Trautmann and O'Rourke (1983) conducted experimental tests on buried pipes in sand and their results were used in this study to examine the capability of the current numerical method. Their physical tests were performed in a tank with 1.2(W)X2.3(L)X1.2(D) m dimensions. The schematic of the test set up is shown in Figure 2.

The Cornell filter sand was used for all physical tests which were clean, sub-angular, fluvioglacial sand having a coefficient of uniformity (C_u) of 2.6 and an effective grain size (D_{10}) of 0.2 mm. The 102 mm pipe was fabricated from ASTM Grade A-36 steel. Soil–pipe interaction was investigated at three different densities of 14.8kN/m^3 (loose), 16.4 kN/m^3(medium), and 17.7 kN/m^3 (dense), corresponding to the relative density of 0%, 45%, and 80%, respectively. In practice, the sand placed around a pipeline is often in the state of medium to dense conditions. Hence, the behavior of these tests in medium and dense sands was simulated using FDM analyses. Two different soil constitutive models were used in the numerical model by Yimsiri et al.(2004) : Mohr-Coulomb model, and Nor-Sand model.

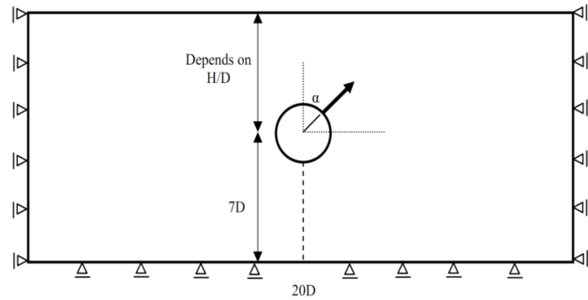

Figure 2. Schematic of a buried pipe

In this study, a different constitutive soil model for the continuous strain hardening-softening and volumetric dilatancy of soils is proposed using finite difference method to simulate the nonlinear behaviour of sand. Strain-hardening/softening constitutive model is based on the Mohr-Coulomb model with non-associated shear and associated tension flow rules. The differences, however, lie in the possibility that the cohesion, friction, dilation and tensile strength may harden or soften after the onset of plastic yield. In the Mohr-Coulomb model those properties are assumed to remain constant. There are four parameters needed to create this model, namely the elastic modulus *E*, bulk modulus *B*, yield function *f*, and plastic potential function *g*. Using the concept of the Hyperbolic Model recommended by Duncan and Chang (1970), the relation between deviatoric stress and axial strain is similar to a hyperbolic curve when the axial strain is smaller than 0.5% to determine the elastic modulus *E*. According to the theory of elasticity, the value of bulk modulus can be expressed as a function of elastic modulus (*E*) and Poisson's ratio (*v*). As shown in Figure 3, all parameters of this model can be expressed as a function of plastic strain. The relations between the parameters have been established by Hsu (2005) and have been used in this study. He conducted many triaxial tests in sands to find best relations functions.

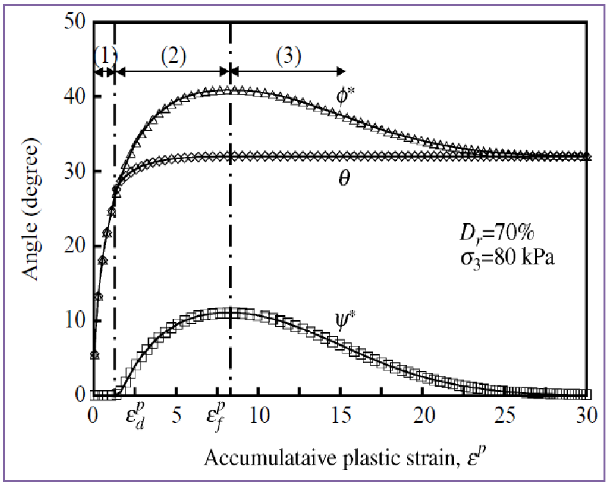

Figure 3. Example of relationship between ψ^*, φ^* and θ versus ε_p of dense sand (Hsu, 2005)

To simulate the experimental soil-pipe model, some actual parameters reported by Trautmann and O'Rourke (1983), are used. The parameters of D_r = 80%, γ = 17.7 kN/m^3 are used for dense sand were then adjusted to conform to the effective vertical stress σ_v' at the center of the pipe for upward pipe movement, for each case of embedment depth. Other input parameters that calculated by Hsu continuous strain hardening-softening strain relationships, are summarized in Table 1.

Table 1. Input soil parameters used for numerical model of soil-pipeline interaction

Direction	Lateral		Upward	
H/D	2	11.5	4	13
B(kPa)	5.26×10^3	7.46×10^3	6.04×10^3	7.64×10^3
G(kPa)	0.63×10^3	2.54×10^3	1.09×10^3	2.80×10^3
ϕ_p	44	44	44	44
ϕ_{cv}	31	31	31	31
$\varepsilon_f{}^p$	0.001	0.001	0.01	0.01
$\varepsilon_c{}^p$	0.035	0.088	0.025	0.066
$\varepsilon_d{}^p$	0.000	0.000	0.000	0.000

The analysis is performed in plane strain and dry conditions. The distance between boundaries is chosen big enough to eliminate the boundary effect. A displacement boundary fixed in x direction is provided on both sides of the grid and a rigid displacement boundary (fixed in x and y direction) is provided at bottom of the grid. By setting initial conditions in the FLAC grid, an attempt is made to reproduce this in-situ state so the soil domain is initially equilibrated to gravity stresses. The interaction between the pipeline and surrounding soil is modeled by an interface element, in which the slip and separation between the pipe and soil is allowed. The pipe is pulled in the lateral (α=90º) and upward (α=0º) directions by imposing displacement boundary conditions to all nodes of the pipe; hence, there is no nodal rotation in the pipeline section due to rigid behaviour.

Some FDM analysis results comparing other previous studies with the current study are shown in Figures 4 and 5 in the form of force–displacement curves for lateral and upward pipe movements, respectively.

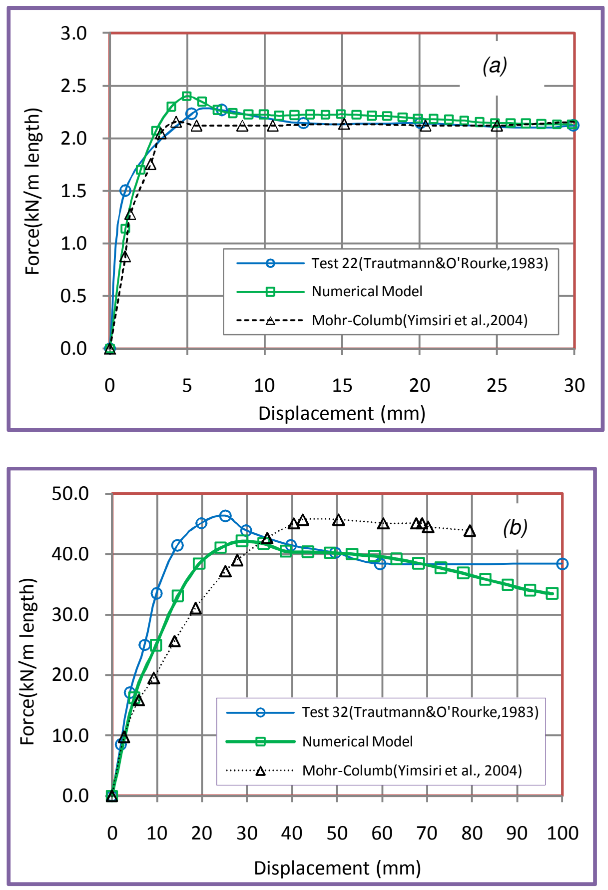

Figure 4. Results of analysis for lateral pipe movement, (a) H/D=2, (b) H/D=11.5

The interface friction angle between the pipe and soil ϕ_m is assumed to be equal to $\phi_p/2$. In fact, this parameter is not easy to evaluate because it depends on the interface characteristics and the degree of relative movement (slip) between pipe and soil. Generally, the pipe surface friction angle ϕ_m ranges from about 20° to a value equal to the friction angle of the soil (e.g. Yoshima and Kishida 1981).

For lateral pipe movement (α=90º), at *H/D* of 2 and 11.5, the FDM results agree both with the experimental data and FE results for dense sand (Figures 4a and 4b) whereas they underestimate the experimental data for medium sand. Also, for upward pipe movement (α=0º), at *H/D* of 4 and 13, the FDM results are in good agreement with the experimental data and FE results for dense sand (Figures 5a and 5b) whereas they underestimate the experimental data for medium sand. It concludes that the numerical model conducted by FLAC 2D v.4.0 and the finite differences method can use for numerical analysis of buried pipes in complex loading. Also, we can monitor many other results of analysis such as soil failure mechanism, displacements of soil and stresses.

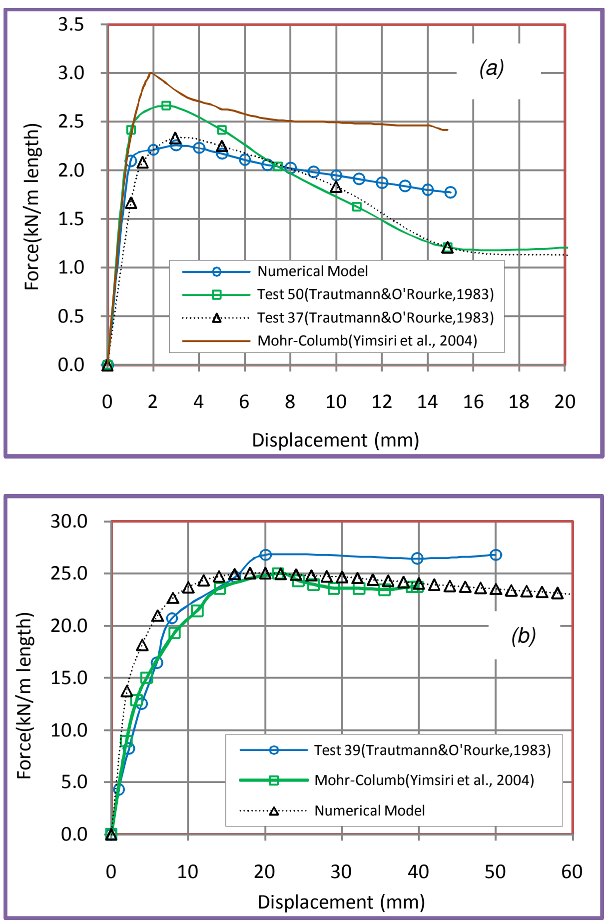

Figure 5. Results of analysis for upward pipe movement, (a) H/D=4, (b) H/D=13

To extend the approach of soil-pipe interaction problems to address the effect of relative pipe–soil movement in the oblique direction where α is not 0 and 90, the analyses were performed with various α values (15º,30º,45º,60º,75º) to find failure envelope. Figure 6 shows the *FLAC* results comparing other failure criterion in terms of loads (p,q), Herein p and q are the horizontal and vertical force components on a pipe and and p_{u0} and q_{u0}=transverse horizontal (α=90º) and transverse vertical (α=0º) ultimate soil resistances per unit length of pipe, respectively.

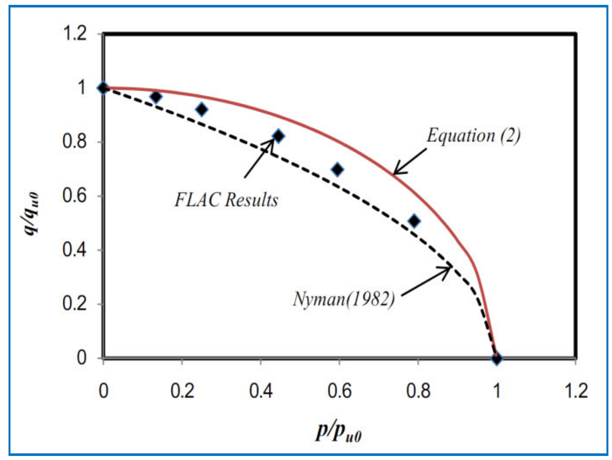

Figure 6. Failure envelopes for pipes under oblique loading buried in sand

As shown above, the transverse load on pipes in each direction in dry sand at ultimate states may be related via:

$$(\frac{P}{P_{u0}})^2 + (\frac{q}{q_{u0}})^2 = 1 \qquad [2]$$

The model performance is further illustrated by failure mechanism of surrounding soil as Figure 7. '*' marks indicates yield places in shear, '×' elements are elastic. Also, the stresses and strains in yield places are bigger than others.

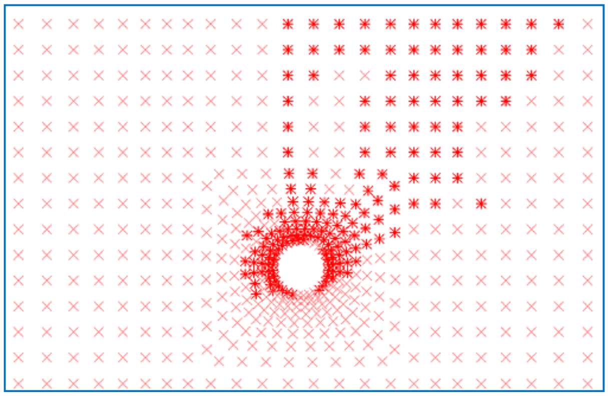

Figure 7. Failure mechanism of surrounding soil with α=15º

5 PARAMETRIC ANALYSIS

This section addresses the scale effect and the influence of burial depth corresponding to various series of models. The influence of soil properties, including dilatancy, strain hardening and pressure dependency, is investigated by changing the parameters used in the soil model.

5.1 Effect of Pipe Diameter

To study the scale effects of pipe diameter on the dimensionless ultimate transverse bearing capacity, N_q, the results of the analysis for different pipe sizes at the same burial depth (*H/D*=5) were grouped together as shown in Figures 8a and 8b for both horizontal and vertical directions buried in medium sand ($\phi_p = 40^\circ$, $\gamma_d = 15\ kN/m^3$).

As shown in Figures 8a and 8b the maximum horizontal dimensionless force, N_{qh}, at a given burial depth ratio varies with pipe diameter *D* but it was found that the changes of the maximum vertical dimensionless force, N_{qv}, are minor and can be neglected. More specifically, N_{qh} decreases from 13.7 to 9.8 when D increases from 0.3 to 2 and N_{qv} changes from 3.9 to 4.1 at *H/D*=5.

5.2 Effect of Burial Depth Ratio

After calibrating the FDM models with the tank experiments as well as the FEM models, pipe loading cases are simulated using the input parameters derived for the various embedment ratios. An example of the computed force-displacement curves are shown in Figure 9 in the case of medium sand ($\phi_p = 40^\circ$, $\gamma_d = 15\ kN/m^3$) where pipe diameter is *D=1m*.

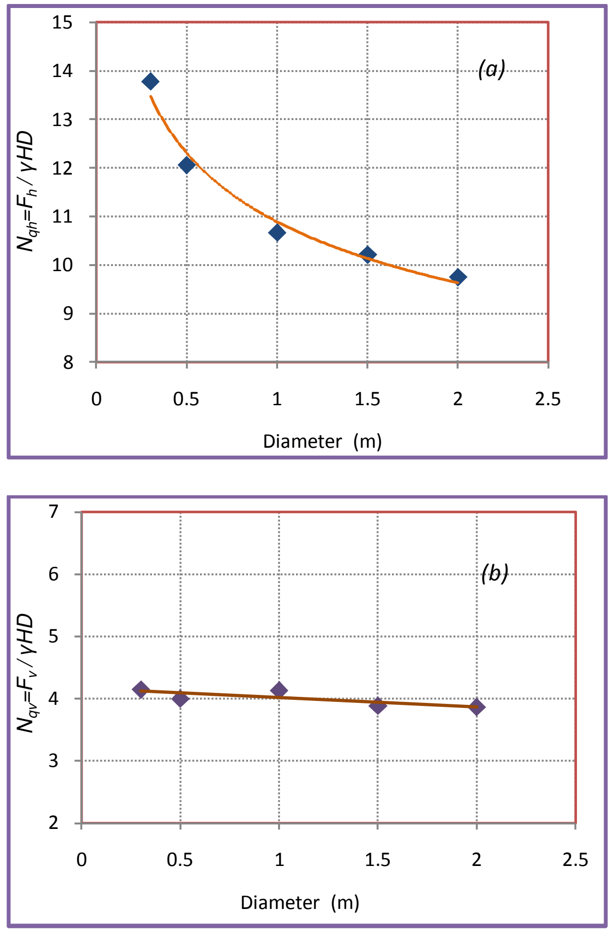

Figure 8. Values of bearing capacity factor for various pipe sizes, (a) horizontal direction, (b) vertical direction

Figure 10 shows the relationship between the peak dimensionless force per unit length of pipe and embedment ratio obtained from the analyses. It is found that the predicted interaction forces increases where burial depth ratio increases or the height of backfill increases. Also, for a given pipe diameter *D*, with the increase of *H/D* ratio, a larger pipe displacement is required to mobilize the maximum soil resistance.

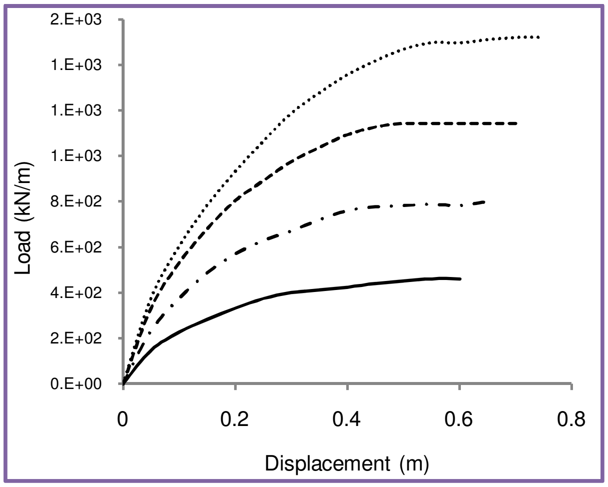

Figure 9. Horizontal force-displacement curve for different burial depth ratios in the medium sand (*D=1m*)

The relation of N_{qh} with burial depth ratio is plotted in figure 10. As maintained on the graph, the value of N_{qh} increases with H/D at shallow conditions (H/D<10). At deeper depths, the displacement pattern of medium sand shows local shear failure around pipe, therefore the failure mechanism is different from that at shallow depths. In order to investigate the effect of burial depth on pipe–soil interactions in the case of deep conditions, the analysis extended to larger *H/D*. The results of analysis to estimate the dimensionless horizontal bearing capacity factor, N_{qh}, from *H/D*=3 to 60 for a rigid pipe *D*=200 mm are produced. Four different cases of sandy soil were proposed for higher *H/D* ratios. Table 2 shows a summary of sand properties.

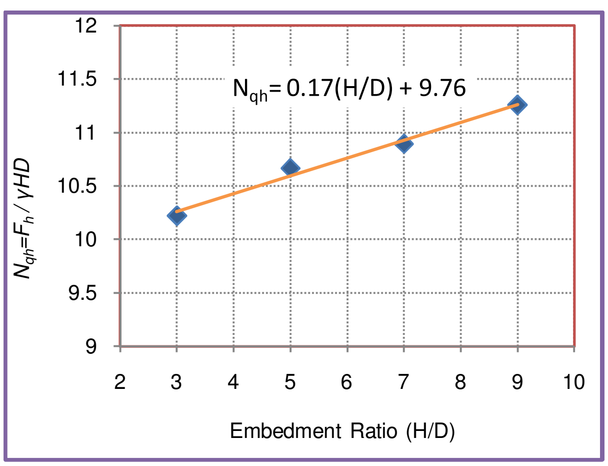

Figure 10. Function of horizontal maximum dimensionless forces versus different burial depth ratios in the medium sand (*D=1m*)

Table 2. Properties of sand used in the analyses for higher *H/D* ratios

Case No.	$\rho(kg/m^3)$	ϕ	ψ	$E(MPa)$
1	1317	32	0	6
2	1500	36	5	15
3	1543	40	10	20
4	1700	44	15	22

Figure 11 shows the dimensionless horizontal bearing capacity factor, N_{qh} plotted against embedment ratios of as large as 60. The results show that, for transverse pipe movements, the peak dimensionless forces increase approximately linearly with the embedment ratios at shallow embedment conditions and reach their maximum values at a certain embedment ratio after which the peak dimensionless forces are approximately constant. The depth at which this transition occurs is called the "critical embedment depth" and the constant peak dimensionless force is termed the "critical peak dimensionless force". For lateral pipe movement, the critical embedment ratio for dry sand is *H/D=15* with the corresponding critical peak dimensionless force of 9 to 20. In all analyses, since the shearing resistance of soil is a function of confining pressure which varies with burial depth, the softening/hardening soil model is more applicable.

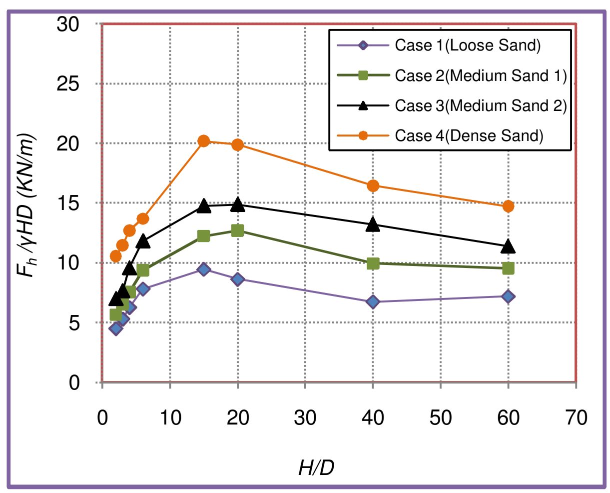

Figure 11. Variation of maximum dimensionless forces with burial depth ratio in the case of deep conditions for sands

6 SUMMARY AND CONCLUSIONS

The results of analyses of soil restraint to transverse movement of pipes in sand are presented. The results of the nonlinear Mohr-Coulomb model to predict the soil restraints to the transverse movement of pipes are presented together with the experimental results. The summary and conclusions of this study are as follows: (1) Soil-pipeline interaction numerical model performed using finite difference method. The predictive capability of strain-softening/hardening constitutive model on sand was demonstrated. (2) The way of lateral and upward interaction is introduced, the pipeline moves against the soil or the soil moves against the pipeline. This affects the stresses and strains and consequently, affects the magnitude of lateral and vertical interaction force as a function of the soil type, pipe size and embedment depth of buried pipe. (3) After calibration the model, analyses extended for oblique direction so the failure envelope expressed and a failure criterion introduced for ultimate state of loads on pipes buried in sand as a function of p_{U0} and q_{u0}. (4) Based on the parametric study, the variation of the maximum dimensionless force N_q with pipe diameter D and burial depth ratio H/D was established. (5) The variation of bearing capacity factor in the horizontal component is a function of the pipe diameter. Therefore for a given burial depth ratio, a pipe with smaller diameter, has a larger ultimate horizontal dimensionless force with no changes in vertical component observed. (6) Although N_q increases with H/D at shallow conditions, the relation is not unique for all depths. Because of the local failure mechanism at large H/D, the variation of N_q is assumed to be zero at deep conditions for pipes buried in sand in both lateral and vertical directions.

7 REFERENCES

Altaee, A. and Boivin, R. 1995. Laterally displaced pipelines: finite element analysis, *Proceedings of 14th International Conference on Offshore Mechanics and Arctic Engineering*, 5: 209-216.

American Lifeline Alliance (ALA) 2005. *Seismic guidelines for water pipelines*.

Audibert, J. M.E. and Nyman, K.J. 1977. Soil restraint against horizontal motion of pipes, *Journal of Geotechnical Engineering Division, American Society of Civil Engineers,* 103(10): 1119–1142.

Bruschi, R., Monti, P., Bolzoni, G. and Tagliaferri, R. 1995. Finite element method as numerical laboratory for analysing pipeline response under internal pressure, axial load, bending moment, *Proceeding of 14th Offshore Mechanics and Arctic Engineering*, OMAE, Houston, TX, USA, Pipeline Technology, 5: 389-401.

C-CORE. 2003. *3D finite element analysis of pipe-soil interaction – effects of groundwater*, Final Report Prepared for Minerals Management Service, C-CORE Report R-02-029-076.

Duncan, J.M. and Chang, C.Y. 1970. Nonlinear analysis of stress and strain in soils, *ASCE, Journal of the Soil Mechanics and Foundation Engineering Division,* 96(SM5): 1629-1653.

Guo, P.G. 2005. Numerical modeling of pipe-soil interaction under oblique loading, ASCE *Journal of Geotechnical Engineering,* 131(2): 260–268.

Hansen, J.B. 1961. *The ultimate resistance of rigid piles against transversal forces*, Bulletin No. 12, Danish Geotechnical Institute, Copenhagen, Denmark, pp. 5–9.

Hsu, S.T. 2005. A constitutive model for the uplift behavior of anchors in cohesionless soils*, Journal of the Chinese Institute of Engineers*, 28(2): 305-317.

Hsu, T., Chen, Y. and Hung, W. 2006. Soil restraint to oblique movement of buried pipes in dense sand, *J. Trans. Eng.*, 132(2): 175–181.

Hurley, S. and Phillips, R. 1999. *Large scale modelling of pipeline/soil interaction under lateral loading,* Final Report. Contract Report for Minerals Management Service, U.S. Department of the Interior, C-CORE Publication, p. 225.

O'Rourke, M., Gadicherla, V. and Abdoun, T. 2004. *Centrifuge modeling of PGD response of buried pipe*.

O'Rourke, M.J. and Liu, X. 1999. *Response of buried pipelines subject to earthquake effects,* MCEER Monograph No. 3.

Popescu, R., Philips, R., Konuk, I. and Deacu, D. 1999. Numerical and physical modeling of pipe-soil interaction*, Proceedings of the 52nd Canadian Geotechnical Conference*, Regina, SK, pp. 437-444.

Trautmann, C.H. and O'Rourke, T.D. 1983. Behavior of pipe in dry sand under lateral and uplift loading, *Geotechnical Engineering Report* 83-7, Cornell University, Ithaca, N.Y.

Winkler E. 1867. *Die leher von der elastizitat und festigkeit. dominicus Prague. Dominicus*, Prague.

Yimsiri, S., Soga, K., Yoshizaki, K., Dasari, R.G. and O'Rourke, T.D. 2004. Lateral and upward soil-pipeline interactions in sand for deep embedment conditions, ASCE *Journal of Geotechnical Engineering,* 130(8): 830–842.

Yoshima, Y. and Kishida, T. 1981. A ring torsion apparatus for evaluating friction between soil and metal surfaces, *Geotechnical Testing Journal, ASTM*, 4(4): 145–152.

Yoshizaki, K. and Sakanoue, T. 2004. Analytical study on soil-pipeline interaction due to large ground deformation, *13th World Conference on Earthquake Engineering*, Vancouver, B.C., Canada, Paper No. 1402.